

Effects of Silicon Impurity on Optical Properties of $\text{Sc}_2\text{C}(\text{OH})_2$ Monolayer: A DFT Study

Reihan Nejatipour* and Mehrdad Dadsetani

Department of Physics, Lorestan University, Khoramabad, Lorestan, Iran

*Corresponding author email: nejati.r@lu.ac.ir

Regular paper: Received: Sep. 07, 2022, Revised: Nov. 15, 2022, Accepted: Nov. 26, 2022,
Available Online: Nov. 28, 2022, DOI: 10.52547/ijop.16.1.99

ABSTRACT— In the density functional theory (DFT), optical properties of $\text{Sc}_2\text{C}(\text{OH})_2$ monolayer are studied with and without silicon impurity. In the presence of silicon impurity, the structure and properties of this compound were changed from a semiconductor with a 0.57 eV band-gap to a topological insulator with a zero band-gap and a band inversion. With and without the silicon impurity, the spectral features in this compound originate from the electron transition from the p-Si and p-C to d-Sc and s-H, respectively. The values of optical constants are increased in the doped-structure with respect to the pure structure.

KEYWORDS: Density functional theory (DFT), Electronic properties, MXenes, Optical properties, $\text{Sc}_2\text{C}(\text{OH})_2$ monolayer, Silicon impurity.

I. INTRODUCTION

After discovering graphene [1], the first two-dimensional (2D) material, scientific researches were conducted to study and synthesize the other possible 2D materials for recompensing the industrial limitations of graphene such as its zero bandgap [2-5]. Efforts led to the discovery of some new 2D materials with interesting and promising properties such as a band gap, gas sensing, absorbing, reflecting, excellent electron mobility, high mechanical strength and flexibility, etc. Hexagonal boron nitride (h-BN) [6], transition metal dichalcogenides (TMDs) [7], stanene [8], silicene [9], germanene [10], phosphorene [11], and 2D organic polymers [12] are 2D compounds used for electronic and photovoltaic applications such as light emitting

diodes, energy storage, lithium-ion batteries, transistors, solar cells and photocatalytic cells.

MXenes are a group of recently discovered 2D materials which have attracted much attention because of their interesting physical properties and their appealing opportunities for practical applications in energy storage systems, electronic devices, catalysts, and spintronics [13,14]. They are extracted by exfoliation of the MAX phase, where M is an early transition metal, A is an element from groups 13 or 14 of the periodic table, such as Ge, Al, or P, and X is nitrogen or carbon [15-17]. By removing the A elements from the MAX phases, the MXene monolayer is created in the form of $\text{Mn}+1\text{Xn}$, and during synthesis, their outer layers are attached to the F, OH, and/or O surface groups, in which case they are represented by the formula $\text{Mn}+1\text{XnTx}$ ($\text{T} = \text{F}, \text{OH}, \text{O}$) [18]. Functional groups in MXenes have a great impact on their appearance as they can change a wide range of different properties for them. Attractive physical properties that are rarely seen in their corresponding MAX phase might be achieved, and this has significantly expanded the range of their potential applications [19,20]. MXenes have tremendous applications in electronics, optics, and optoelectronics [21]. Pristine MXenes are generally metals whose band gaps can be engineered by strain or functionalizing. Among them, the Sc_2C monolayer has a band gap of about 0.45-1.80 eV after OH, F, or O surface functionalization. The $\text{Sc}_2\text{C}(\text{OH})_2$ monolayer is a semiconductor with a direct band gap of 0.58 eV. This compound is a topological insulator in

the presence of silicon or germanium impurities [22]. This motivated us to study the physical properties of Si-doped $\text{Sc}_2\text{C}(\text{OH})_2$ monolayer.

Industrial applications of materials need the knowledge of their electronic and optical properties. Despite the importance of optical properties and related applications in photocatalysts and optoelectronic devices, they have not been widely studied by researchers. The optical properties of $\text{Sc}_2\text{C}(\text{OH})_2$ in the presence of impurities such as silicon have not been investigated in any study. The present study is a compensation for this shortcoming by detecting the optical response of doped $\text{Sc}_2\text{C}(\text{OH})_2$, and it paves the way for future studies. First, the electronic properties of the ground state for the pristine and doped $\text{Sc}_2\text{C}(\text{OH})_2$ MXene are obtained in the framework of density functional theory. Next, using the random phase approximation (RPA), the present study calculates and compares and contrasts the optical spectra including the real ($\epsilon_1(\omega)$) and imaginary ($\epsilon_2(\omega)$) parts of the dielectric function, energy loss spectra, reflectivity, refraction, and extinction functions of Si-doped $\text{Sc}_2\text{C}(\text{OH})_2$.

II. COMPUTATIONAL DETAILS

The method of calculations is full potential linearized augmented plane wave (FPLAPW) implemented in the WIEN2k code [23], in which no approximation is used for calculating the crystal potential. The cutoff parameter for the basis set, RMTKMax, is set in 4.0, where RMT is the radius of the smallest atom in crystal, and KMax is the maximum wave vector in inverse space. The exchange-correlation potential within the generalized gradient approximation (GGA) is calculated by means of Perdew, Burke and Ernzerhof (PBE) functional [24]. The maximum of quantum number lMax for expanding of wave functions inside the atomic spheres is set as 10, and the GMax parameter, the maximum vector in inverse space is taken to be 14 Bohr⁻¹. Brillouin zone (BZ) integrations within self-consistency cycles are performed via a tetrahedron method, containing 14 (10×10×1) and 5 (5×5×1) k-points in the irreducible BZ of pure and Si-

doped $\text{Sc}_2\text{C}(\text{OH})_2$, respectively. In order to take the impurity into account, a single carbon atom in a 3×3×1 supercell is replaced by a silicon atom. The lattice and internal parameters of both pure and Si-doped monolayers are optimized up to a force convergence of 1.0 mRy/a.u.

The imaginary part ($\epsilon_2(\omega)$) of the dielectric functions is calculated in the RPA as [25]:

$$\begin{aligned} \epsilon_2(\omega) &= \frac{Ve^2}{2\pi\hbar m^2 \omega^2} \int d^3k \sum_{nn'} |\langle kn|p|kn' \rangle|^2 f(kn) \\ &\times (1 - f(kn')) \delta(E_{kn} - E_{kn'} - \hbar\omega), \end{aligned} \quad (1)$$

where V is the crystal volume, p is the momentum operator, $\hbar\omega$ is the photon energy, $|kn\rangle$ and E_{kn} are the eigenfunction and the eigenenergy, and $f(kn)$ is the Fermi distribution function. The RPA only considers the direct electron transitions from the valence bands to the conduction ones, and the indirect transitions which occur by the phonons are neglected since they have a negligible effect on the optical spectra. The real part of the dielectric function can be obtained by the Kramers-Kronig transformations, and the other optical spectra are reached by the full complex dielectric function [25].

III. RESULTS AND DISCUSSION

A. Structural and electronic properties

Figure 1 displays the crystal structure of $\text{Sc}_2\text{C}(\text{OH})_2$ monolayer. The Sc-C bond length in pure structure is 2.28 Å, whereas the Sc-Si in the doped structure is 2.476 Å. These values are in accordance with the other study as it has reported Sc-C and Sc-Si bond lengths as 2.283 and 2.471 Å, respectively [22].

The Sc-C-Sc bond angle is 87.574° in the pristine monolayer, while Sc-Si-Sc bond angle is 86.242° in doped monolayer.

The analysis of the densities of states (DOS) and the band structure of $\text{Sc}_2\text{C}(\text{OH})_2$ in Fig. 2 shows that this monolayer is a semiconductor with the 0.57 eV energy band gap which is in

accordance with the existing computational report [22]. According to the DOS plot of the pure structure and the band character analysis, the main orbital contributions in the valence band maximum states consist of p-C and d-Sc, and the lowest conduction band is composed of s-H orbitals. The lowest unoccupied state has a parabolic behavior reminiscent of the free electron band structure.

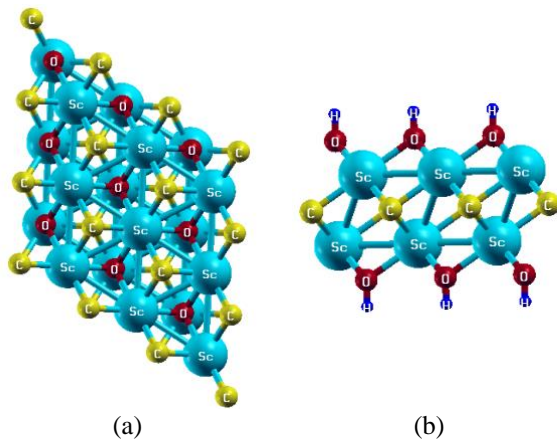


Fig. 1. The top (a) and side (b) views of a 3×3 supercell of $\text{Sc}_2\text{C}(\text{OH})_2$ monolayer.

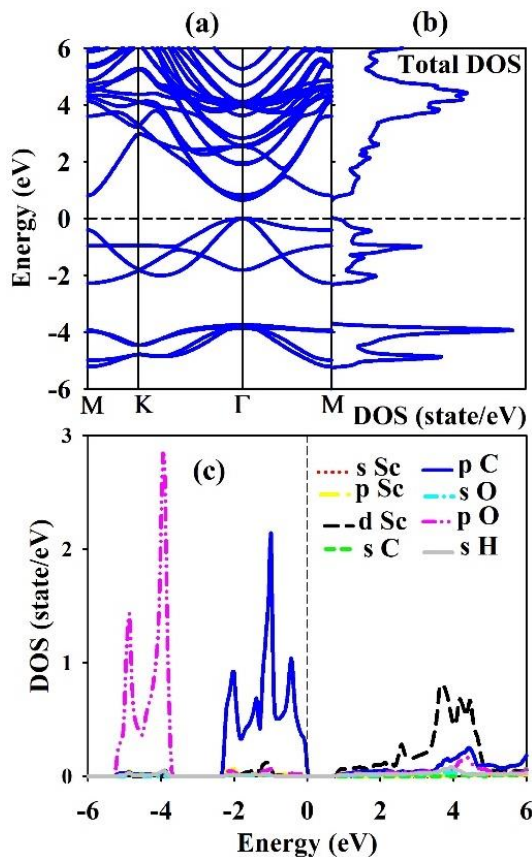


Fig. 2. (a) Band structure, (b) Total DOS, and (c) partial DOS of pure $\text{Sc}_2\text{C}(\text{OH})_2$ monolayer.

As Fig. 3 shows, the presence of silicon changes this procedure. In the doped structure, p orbitals of impurity atom (Si) have the main contribution in the valence band. Furthermore, the energy band gap decreases to zero, which means the p-Si states result in the increase energy of the highest occupied state. The unoccupied surface states of s-H in the lowest conduction band of the pure structure come to the second unoccupied state above the Fermi level of the doped structure. Now in the doped structure, the Sc-C-Si states play the main role as the lowest unoccupied surface states. Therefore, a band movement at the Γ point near the Fermi level is obvious, which these properties introduce the Si-doped $\text{Sc}_2\text{C}(\text{OH})_2$ as a topologic insulator.

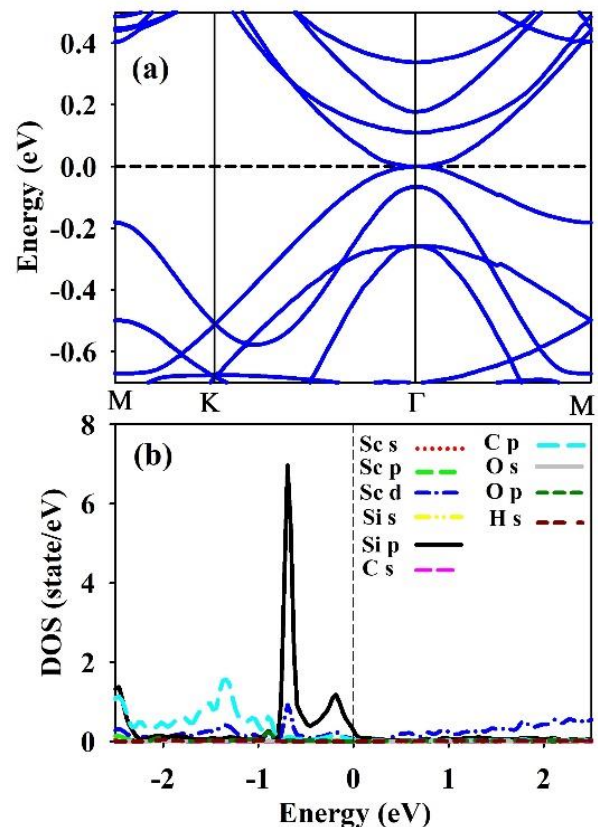


Fig. 3. (a) Band structure and (b) partial DOS of silicon-doped $\text{Sc}_2\text{C}(\text{OH})_2$ monolayer. Band inversion occur at the Γ point near the Fermi level.

B. Optical properties

In the following, optical properties of $\text{Sc}_2\text{C}(\text{OH})_2$ with and without silicon impurity are compared and contrasted. Due to the hexagonal symmetry, optical spectra of $\text{Sc}_2\text{C}(\text{OH})_2$ have two independent components: xx and zz. According to Fig. 4, dielectric

constants ($\epsilon_1(\omega=0)$) of pure $\text{Sc}_2\text{C}(\text{OH})_2$ in the x and z directions are 4.63 and 3.36. For the Si-doped structure, these values increase to 7.77 and 4.08. A comparison of the overall trends of the spectra shows that adding impurity causes a blue (red) shift in the xx (zz) spectra. In addition, anisotropy is obvious in the optical spectra.

The analysis of the band structure and the densities of states shows that the spectral features in the $\epsilon_2(\omega)$ originate from electron transition of the p orbital of carbon atom to the d orbital of scandium and mainly the s orbital of hydrogen atoms. The same analysis confirms that in the doped monolayer, the main contribution of the electron transitions is from the p orbital of silicon atom to the d orbital of scandium and s orbital of hydrogen atoms.

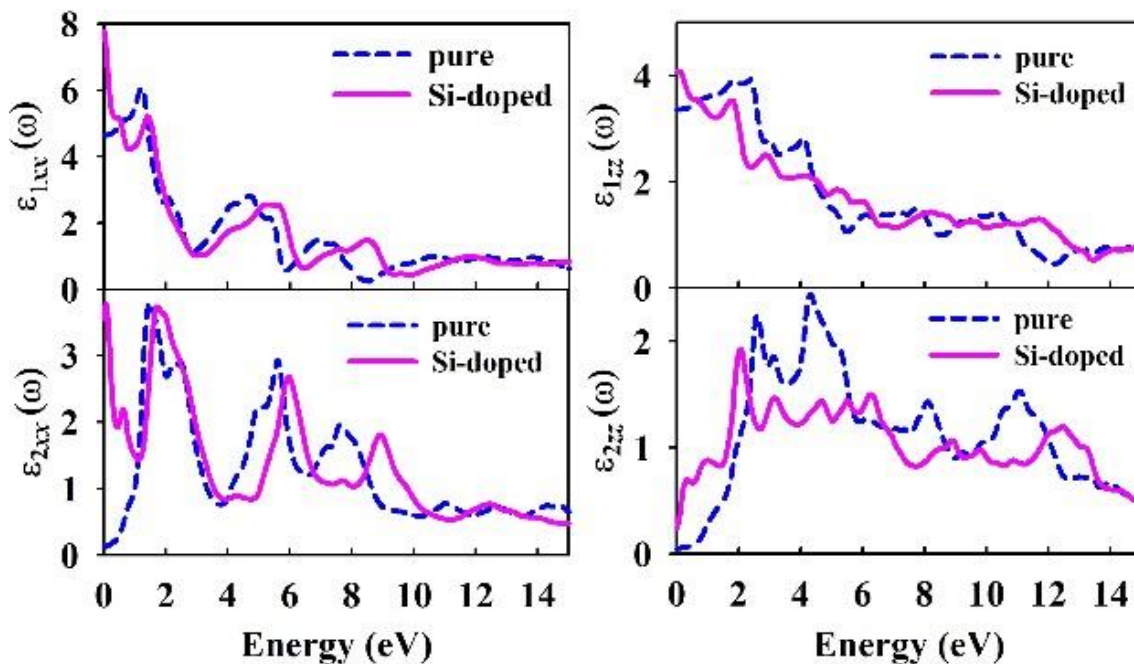


Fig. 4. xx-(left) and zz-components (right) of real (top) and imaginary (bottom) parts of the dielectric functions of pure (dashed lines) and silicon-doped (solid lines) $\text{Sc}_2\text{C}(\text{OH})_2$ monolayer.

The electron energy loss function which means the energy loss function of an electron beam transmitted from the material, is defined as the equation $L(\omega) = -\text{Im}(1/\epsilon(\omega))$, and so, it depends on the response function of the material. Each spectral feature of loss function, originating from interband transitions, can be attributed to the corresponding feature in the dielectric function (Figs. 4 and 5). Therefore, in both xx and zz components of the energy loss function of pure monolayer, the first main peaks at the energies of 2.33 and 5.91 eV originate from interband electron transitions.

The corresponding features in the Si-doped monolayer occur at the higher energies of 2.45 and 6.05 eV. For the small values of the dielectric function, a main peak appears in the loss function as the plasmon peak belonging to

the energy loss of some transmitted electrons which cause the plural exciting of the charge density of material. The main spectral features in the xx and zz components of $L(\omega)$ of pure (doped) $\text{Sc}_2\text{C}(\text{OH})_2$ occur at the energies of 8.55 and 12.17 eV (9.37 and 13.42 eV) as plasmonic features, respectively. Therefore, compared to the pure monolayer, the main spectral features in the doped monolayer occur at the higher energies. A blue shift in the loss function of Si-doped structure can be attributed to the band movement near the Fermi level. Since the s orbital of hydrogen atom shifts from the lowest conduction band in the pure structure to the second lowest conduction band at the higher energies in the Si-doped ones, the spectral features in the loss function for the doped structure occur at higher energies.

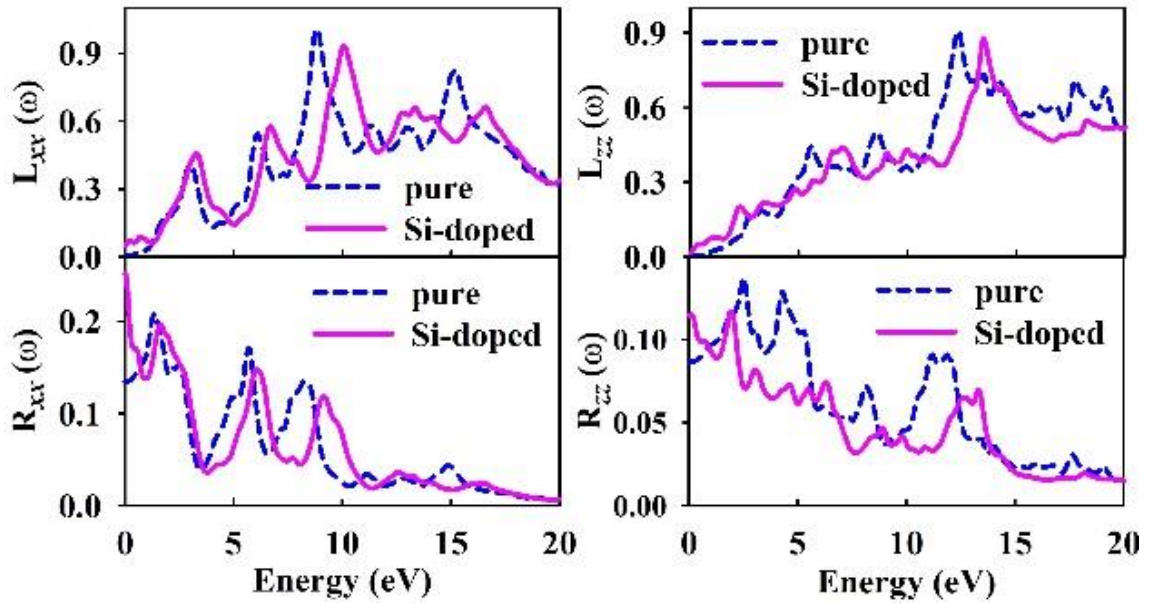


Fig. 5. xx-(left) and zz-components (right) of energy loss (top) and reflectivity (bottom) functions of pure (dashed lines) and silicon-doped (solid lines) $\text{Sc}_2\text{C}(\text{OH})_2$ monolayer.

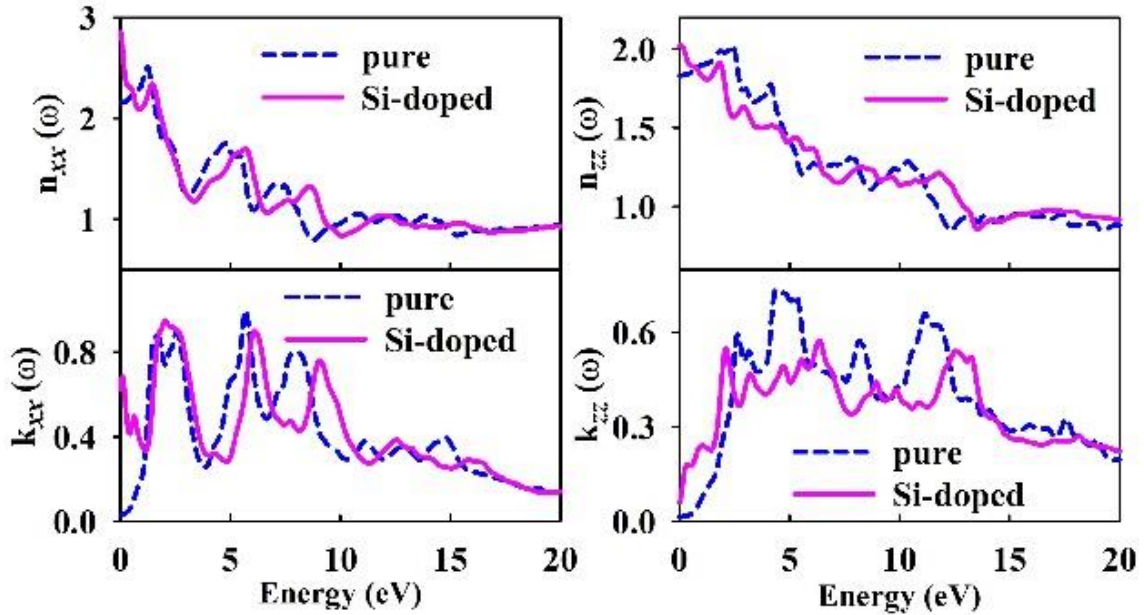


Fig. 6. xx-(left) and zz-components (right) of refraction (top) and extinction (bottom) functions of pure (dashed lines) and silicon-doped (solid lines) $\text{Sc}_2\text{C}(\text{OH})_2$ monolayer.

Figure 5 shows that the maximum reflection for pure monolayer occurs at the energies of 1.30 and 2.37 eV for xx and zz components, respectively. Corresponding values for the doped monolayer are energies of 0.06 and 1.91 eV, and so, the reflectivity spectrum of doped monolayer tends to the lower energies, since the energy band gap of Si-doped structure is less than that of pure structure (zero vs. 0.57 eV).

According to Fig. 6, for xx and zz components in the pristine $\text{Sc}_2\text{C}(\text{OH})_2$, the static refraction indexes ($n(\omega=0)$) are 2.15 and 1.83,

respectively. These indexes are 2.85 and 2.02 in the doped $\text{Sc}_2\text{C}(\text{OH})_2$. This analysis shows that the static refraction index of $\text{Sc}_2\text{C}(\text{OH})_2$ increases in the presence of silicon impurity.

Another optical function is the extinction coefficient ($k(\omega)$) indicating the amount of the absorption of electromagnetic radiation by the material, in a way that, if the electromagnetic wave easily transmits from the material, the extinction coefficient will be low; otherwise, the coefficient will be high. The main spectral peaks in the xx and zz components of the $k(\omega)$

of pristine $\text{Sc}_2\text{C}(\text{OH})_2$ occur at the energy positions of 5.61 and 4.46 eV, while in the doped structure, they occur at the energy positions of 2.02 and 6.24 eV, respectively. Therefore, the electromagnetic wave at the mentioned frequencies hardly penetrates in the pristine and doped $\text{Sc}_2\text{C}(\text{OH})_2$.

IV. CONCLUSION

With silicon injection in the $\text{Sc}_2\text{C}(\text{OH})_2$ monolayer, the p orbital of the carbon atom in the valence band is replaced by the p orbital of the impurity atom, and a band displacement occurs at the Fermi level. These changes cause the change in the optical response of the studied material. In addition to the spectral moving of energy peak positions, the interaction of electromagnetic beam with the studied material leads to the electron transitions from the p states of carbon atom in pristine $\text{Sc}_2\text{C}(\text{OH})_2$ and the p states of the silicon atom in doped structure to the d states of scandium and s states of hydrogen atoms. Furthermore, the static optical functions mainly increase from the pristine to Si-doped $\text{Sc}_2\text{C}(\text{OH})_2$.

REFERENCES

- [1] K.S. Novoselov, A.K. Geim, S.V. Morozov, D. Jiang, Y. Zhang, S.V. Dubonos, I.V. Grigorieva, and A.A. Firsov, "Electric field effect in atomically thin carbon films," *Science*, Vol. 306, pp. 666-669, 2004.
- [2] D. Singh, S.K. Gupta, Y. Sonvane, and Igor Lukačević, "Antimonene: a monolayer material for ultraviolet optical nanodevices," *J. Mater. Chem. C*, Vol. 4, pp. 6386-6390, 2016.
- [3] A. Karaei Shiraz, A. Yazdanpanah Goharrizi, and S.M. Hamidi "The electronic and optical properties of armchair germanene nanoribbons," *Phys. E: Low-dimension. Sys. Nanostruct.*, Vol. 107, pp. 150-153, 2019.
- [4] A. Karaei Shiraz and A. Yazdanpanah Goharrizi, "Optical properties of buckled bismuthine," *Phys. Status Solidi B* Vol. 257, pp. 1900408-1900412, 2020.
- [5] Y. Xu, B. Peng, H. Zhang, H. Shao, R. Zhang, and H. Zhu, "First-principle calculations of optical properties of monolayer arsenene and antimonene allotropes," *Ann. Phys.* Vol. 529, pp. 1600152 (1-9), 2017.
- [6] H. Wang, Y. Zhao, Y. Xie, X. Ma, and X. Zhang, "Recent progress in synthesis of two-dimensional hexagonal boron nitride," *J Semiconduct.*, Vol. 38, pp. 031003 (1-14), 2017.
- [7] K.F. Mak, C. Lee, J. Hone, J. Shan, and T.F. Heinz, "Atomically Thin MoS_2 : A New Direct-Gap Semiconductor" *Phys. Rev. Lett.*, Vol. 105, pp. 136805 (1-4), 2010.
- [8] C.X. Zhao and J.F. Jia "Stanene: A good platform for topological insulator and topological superconductor," *Front. Phys.* Vol. 15, pp. 53201 (1-15), 2020.
- [9] M.A. Kharadi, G.F.A. Malik, F.A. Khanday, K.A. Shah, S. Mittal, and B.K. Kaushik "Silicene: From Material to Device Applications," *ECS J. Solid State Sci. Technol.* Vol. 9, pp. 115031 (1-20), 2020.
- [10] M.E. Dávila, L. Xian, S. Cahangirov, A. Rubio, and G.L. Lay, "Germanene: a novel two-dimensional germanium allotrope akin to graphene and silicene," *New J. Phys.* Vol. 16, pp. 095002 (1-10), 2014.
- [11] H. Liu, A.T. Neal, Z. Zhu, Z. Luo, X. Xu, D. Tománek, and P.D. Ye, "Phosphorene: An Unexplored 2D Semiconductor with a High Hole Mobility," *ACS Nano*, Vol. 8, pp. 4033-4041, 2014.
- [12] Y. Chen, A. Star, and S. Vidal, "Sweet carbon nanostructures: carbohydrate conjugates with carbon nanotubes and graphene and their applications," *Chem. Soc. Rev.*, Vol. 42, pp. 4532-4542, 2013.
- [13] R. Momeni Feili, M. Dadsetani, R. Nejatipour, and A. Ebrahimian, "Electron Energy Loss Structures of Terminated Scandium and Hafnium MXene Monolayers from First-Principles Calculations," *J. Elec. Mater.* Vol. 49, pp. 2502-2520, 2020.
- [14] M. Naguib, M. Kurtoglu, V. Presser, J. Lu, J. Niu, M. Heon, L. Hultman, Y. Gogotsi, and M. W. Barsoum, "Two-Dimensional Nanocrystals Produced by Exfoliation of Ti_3AlC_2 ," *Adv. Mater.* Vol. 23, pp. 4248-4253, 2011.
- [15] M.W. Barsoum, "The $\text{M}_{\text{N}+1}\text{AX}_\text{N}$ phases: A new class of solids: Thermodynamically stable nanolaminates," *Prog. Solid State Chem.* Vol. 28, pp. 201-281, 2000.
- [16] Z.M. Sun, "Progress in research and development on MAX phases: a family of

- layered ternary compounds,” *Int. Mater. Rev.* Vol. 56, pp. 143-166, 2011.
- [17] M. Khazaei, M. Arai, T. Sasaki, M. Estili, and Y. Sakka, “Trends in electronic structures and structural properties of MAX phases: a first-principles study on M_2AlC ($M = Sc, Ti, Cr, Zr, Nb, Mo, Hf$, or Ta), M_2AlN , and hypothetical M_2AlB phases,” *J. Phys.: Condens. Matter*, Vol. 26, pp. 505503 (1-12), 2014.
- [18] M.R. Lukatskaya, O. Mashtalir, C.E. Renyohan, Y. Dallagnese, P. Rozier, P.L. Taberna M. Naguib, P. Simonmichel W. Barsoum, and Y. Gogotsi, “Cation Intercalation and High Volumetric Capacitance of Two-Dimensional Titanium Carbide,” *Science*, Vol. 341, pp. 1502-1505, 2013.
- [19] M. Khazaei, M. Arai, T. Sasaki, C. Y. Chung, N. S. Venkataramanan, M. Estili, Y. Sakka, and Y. Kawazoe, “Novel Electronic and Magnetic Properties of Two-Dimensional Transition Metal Carbides and Nitrides,” *Adv. Funct. Mater.*, Vol. 23, pp. 2185-2192, 2013.
- [20] H. Zhang, G. Yang, X. Zuo, H. Tang, Q. Yanga, and G. Li, “Computational studies on the structural, electronic and optical properties of graphene-like MXenes (M_2CT_2 , $M = Ti, Zr, Hf$; $T = O, F, OH$) and their potential applications as visible-light driven photocatalysts,” *J. Mater. Chem. A*, Vol. 4, pp. 12913-12920, 2016.
- [21] H. Lashgari, M.R. Abolhassani, A. Boochani, S.M. Elahi, and J. Khodadadi, “Electronic and optical properties of 2D graphene-like compounds titanium carbides and nitrides: DFT calculations,” *Solid State Commun.*, Vol. 195, pp. 61-69, 2014.
- [22] E. Balci, Ü.Ö. Akkuş, and S. Berber, “Doped $Sc_2C(OH)_2$ MXene: new type s-pd band inversion topological insulator,” *J Phys. Condens. Matter.*, Vol. 30, pp. 155501 (1-12), 2018.
- [23] P. Blaha, K. Schwarz, F. Tran, R. Laskowski, G.K.H. Madsen, and L.D. Marks, “WIEN2k: An APW+lo program for calculating the properties of solids,” *J. Chem. Phys.*, Vol. 152, pp. 074101 (1-30), 2020.
- [24] J.P. Perdew, K. Burke, and M. Ernzerhof, “Generalized gradient approximation made simple,” *Phys. Rev. Lett.*, Vol. 77, pp. 3865-3868, 1996.
- [25] C. Ambosch-Draxl and J.O. Sofo, “Linear optical properties of solids within the full-potential linearized augmented planewave method,” *Comp. Phys. Commun.*, Vol. 175, pp. 1-14, 2006.



Reihan Nejatipour was born in Khoramabad, Iran, on June 22, 1985. She received the BSc and MSc degrees in Solid State Physics in 2007 and 2010, respectively, from Lorestan University, Khoramabad, Lorestan, Iran. In 2015, she obtained the PhD degree in Solid State Physics from Lorestan University. She is Assistant Professor at Lorestan University from 2020 up to now.



Mehrdad Dadsetani was born in Khoramabad, Iran, on September 1972. He received the BSc and MSc degrees in Solid State Physics in 1995 and 1998, respectively, from Birjand University and Isfahan University of Technology, Iran, respectively. In 2006, he obtained the Ph.D. degree in Solid State Physics from Isfahan University. He was Research Fellow in the field of Condensed Matter Physics from 2006 to 2007 at the University of Antwerp of Belgium. At 2016, he received the degree of full professor at Condensed Matter Physics.

THIS PAGE IS INTENTIONALLY LEFT BLANK.